Applied Energy xxx (2016) xxx–xxx

Contents lists available at ScienceDirect

Applied Energy

journal homepage: www.elsevier.com/locate/apenergy

Effects of silicon carbide MOSFETs on the efficiency and power quality of a microgrid-connected inverter

Xiaofeng Ding, Feida Chen *, Min Du, Hong Guo, Suping Ren

School of Automation Science and Electrical Engineering, BeiHang University, Beijing 100191, China

HIGHLIGHTS

- The characteristics comparison between SiC-inverter and Si-inverter is implemented, considering thermal effects.
- The voltage distortion of inverters is modeling from the perspective of the behaviors of the device.
- The efficiency of the microgrid-connected inverter has been greatly increased by replacing Si with SiC.
- The SiC microgrid-connected inverter has smaller voltage distortion and less harmonic current than those of Si-inverter.
- The proposed analytical model has been validated by the experimental test.

ARTICLE INFO

Article history:
Received 27 July 2016
Received in revised form 18 September 2016
Accepted 1 October 2016
Available online xxxx

Keywords:
Microgrid
Silicon carbide (SiC)
Inverter
Power losses
Current harmonics

ABSTRACT

With the expanding power demands and increasing use of renewable energy resources, microgrids have been widely supported. Wide bandgap semiconductor devices with higher blocking voltage capabilities and higher switching speeds, such as silicon carbide (SiC) devices, will become a critical component in building microgrids. This paper describes a comprehensive investigation of the effects of SiC Metal-Oxide-Semiconductor Field-Effect Transistors (MOSFETs) on the efficiency and power quality of the inverters used in low voltage microgrids compared with conventional inverters based on silicon (Si) Insulated-gate Bipolar Transistors (IGBTs). First, the characteristics of both SiC and Si are measured by a double pulse test (DPT), considering thermal effects. Then, conduction and switching losses under different temperatures are calculated based on DPT results. Second, phase voltage distortions are modeled and calculated according to the tested switching and conduction characteristics of SiC, resulting in harmonic components in the phase current. Finally, an experiment is implemented. The experimental results show that the SiC-inverter greatly increases the energy efficiency and improves the power quality in the microgrid; these results are consistent with the analytical results.

1. Introduction

To address the two urgent goals of protecting the environment and achieving energy sustainability, it is of strategic significance to develop electric vehicles and the distributed energy storage technology [1,2]. Microgrids are an emerging concept for utilizing distributed power generators that gather or aggregate distributed energy resources and loads locally. Microgrids are increasing in popularity because of their inherent advantage in integrating renewable energy sources (RESs), such as solar, wind and waves [3]. Because of the increasing number of RESs that are emerging and being connected to microgrids, the power electronics play a more important role, as shown in Fig. 1 [4]. In such power electronic converters for RESs, particularly in grid-connected inverters, efficiency, power quality and cost are key factors [5].

1.1. Literature review

To attain high efficiency, numerous methodologies have been developed, including developing different topologies of inverters and proposing intelligent control strategies [6–10]. Recently, researchers have performed a large amount of valuable work regarding transformerless topologies for grid-connected inverters and corresponding control strategies that are more efficient than the transformer ones [8–10].

In addition to the different topologies, an increasing number of grid-connected inverters adopt wide bandgap (WBG) devices such

* Corresponding author.
E-mail addresses: dingxiaofeng@buaa.edu.cn (X. Ding), dage820@buaa.edu.cn (F. Chen), dumin@buaa.edu.cn (M. Du), guohong@buaa.edu.cn (H. Guo), rsp93_4@126.com (S. Ren).

http://dx.doi.org/10.1016/j.apenergy.2016.10.011
0306-2619/

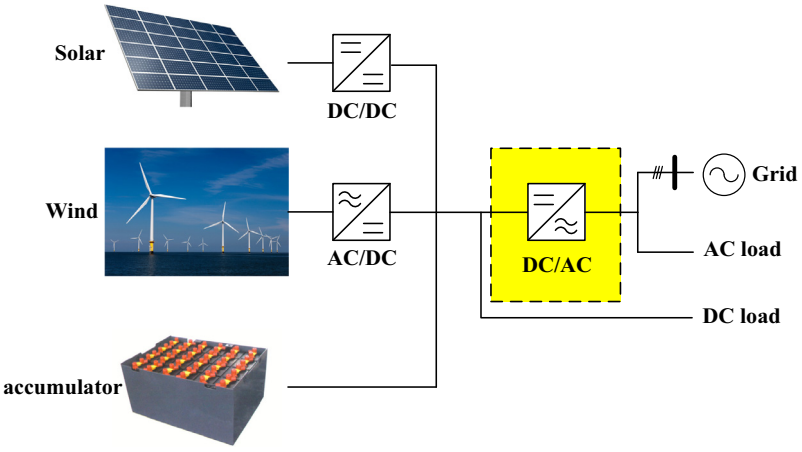

Fig. 1. Schematic illustration of a typical microgrid structure.

as silicon carbide (SiC). Kranzer et al. [11] presented the implementation and performance of 1200 V/30 A normally off SiC-Junction Field-Effect Transistors (JFETs) in photovoltaic inverters (PV-inverters). The characteristics of SiC-JFET are similar with SiC-Insulated-gate Bipolar Transistors (MOSFETs) due to the fact that SiC-JEFT and SiC MOSFET manufactured by the same material of SiC. The SiC-JFETs' low switching energy and on-resistance led to an improvement in efficiency and reduction in the cost and weight of PV-inverters. Rabkowski et al. [12] proposed connecting ten SiC-JFETs in parallel in each position to achieve a very low conduction loss; additionally, a novel gate-drive method was applied, forcing the devices to switch very fast, resulting in very low switching losses. Burger et al. [13] showed that with SiC MOSFETs, it is possible to reduce the production cost and increase the efficiency of PV-inverters. The maximum efficiency of a standard three-phase inverter could be improved from 95.7 to 97.8% just by replacing standard Insulated-gate Bipolar Transistors (IGBTs) with SiC-MOSFETs.

Though the improved efficiency of SiC-inverters is proved through simulations and experiments, the losses of SiC MOSFETs have not been investigated systematically from the perspective of measured intrinsic characteristics. In addition, it is known that the temperature affects switching and conduction behaviors. Therefore, this paper comprehensively investigates the switching and conduction losses of SiC in terms of its intrinsic characteristics, taking thermal effects into account.

Furthermore, a power quality analysis of SiC-inverters stemming from its behavior is also absent in the literature. According to the council of European energy regulators (CEER), the voltage/current harmonic components are one of the main power quality problems in microgrids [14,15]. Harmonic currents induced by nonlinear loads, such as switched mode power supplies (SMPS), variable speed electrical machines, and power electronic inverters, are applicable to microgrids. The presence of power electronic devices in microgrid-connected inverters injects harmonic currents, resulting in excessive transmission and component losses, overheating, malfunctioning of protection relays and interruption of communication [16]. To protect the microgrid against power quality problems, some standards define acceptable thresholds for voltage/current harmonic distortion [17,18].

Palizban et al. [19] reviewed some of the existing microgrid power quality improvement methodologies in the literature. The power quality could be maintained by grid-inverters [20]. Li et al. [21,22] proposed optimally controlled shunt and series inverters. Such a conversion can generate reactive power, supplying reactive loads in dealing with the generation of harmonic currents. In addition to the inverter, active power filters (APFs) are also effective elements for enhancing power quality [23–26]. Chakraborty et al. [24] and Khadem et al. [25] used active filters, and Tzung-Lin and Po-Tai [26] adopted cooperative harmonic filtering.

Although numerous researchers have proposed a variety of valuable methodologies to suppress current harmonics, no one has systematically investigated the current harmonics induced by SiC-inverters in terms of the characteristics of the device. Therefore, this paper investigates the effect of SiC on efficiency as well as on the power quality of microgrid-connected inverters.

1.2. Motivation and innovation

The microgrid-connected inverter is one of the key components in the microgrid as the inverter is connected directly with grid and AC load. The power quality and efficiency of the inverter are vital for the grid and AC load. Hence, this paper presents comprehensive comparisons between SiC- and Si-based microgrid-connected inverters, particularly from the perspectives of efficiency and power quality. The characteristics of both SiC and Si are tested through a double pulse test (DPT) that considers temperature first. Consequently, analytical models of losses for SiC (or Si) based inverters are developed according to the switching and conduction behaviors of devices, taking thermal effects into account. Additionally, the analytical models are validated by experiments. In the experiments the losses are measured directly based on a power analyzer. Then, the voltage distortion and current harmonics caused by SiC and Si inverters are investigated through analytical and experimental methods, which also take the temperature into account.

1.3. Organization of the paper

This paper is organized in the following manner: Section 2 implements the DPT on both SiC and Si to assess their characteristics. Section 3 calculates the power losses of microgrid-connected SiC and Si inverters. Section 4 analyses the output phase voltage distortions and quantitative calculation for both SiC and Si inverters. In Section 5, experimental results are presented to validate the analytical results. Conclusions are drawn in Section 6.

2. Characteristics tests of two devices

A three phase inverter has been selected in order to compare the impact of using SiC MOSFET and Si IGBT. The simplified schematic of an inverter is shown in Fig. 2. A typical photovoltaic inverter system includes a solar panel, a DC-DC converter, a DC-

Please cite this article in press as: Ding X et al. Effects of silicon carbide MOSFETs on the efficiency and power quality of a microgrid-connected inverter. Appl Energy (2016), http://dx.doi.org/10.1016/j.apenergy.2016.10.011

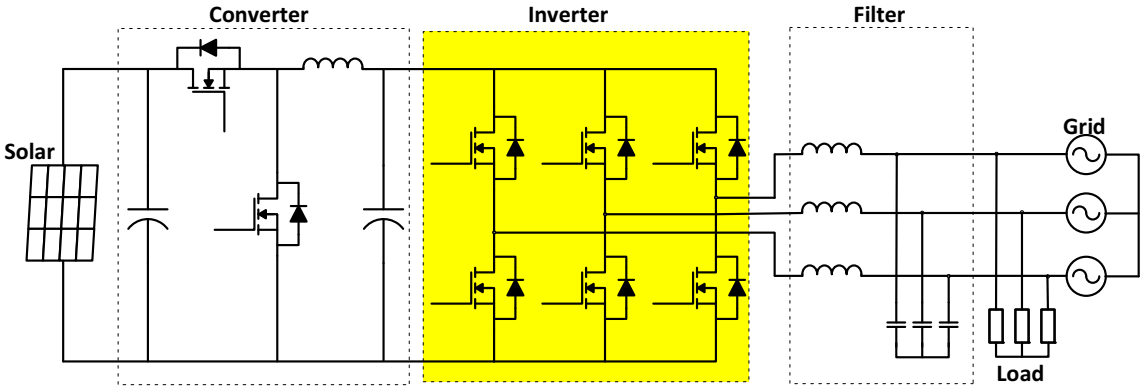

Fig. 2. Simplified schematic of inverter.

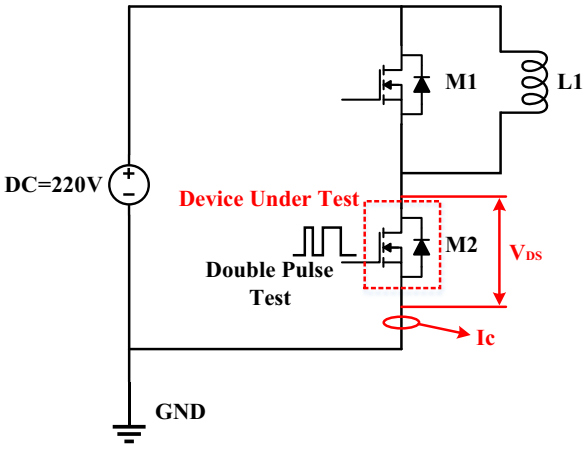

(a)

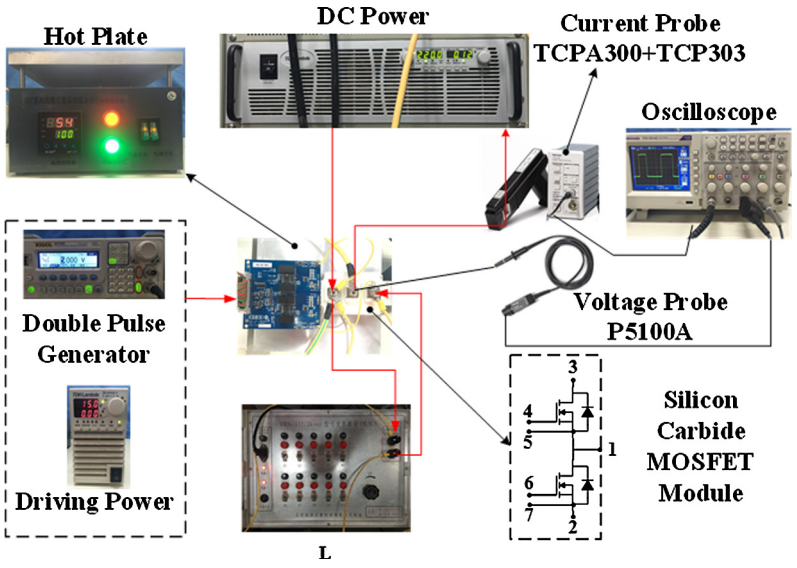

(b)

Fig. 3. DPT test bench. (a) Simplified DPT circuit and (b) actual components in the test bench.

AC inverter, an output filter and an AC load. The inverter based on a Cree 1200 V 300 A SiC MOSFET (CAS300M12BM2) will be investigated and compared with that based on an Infineon 1200 V 400 A Silicon IGBT (FF400R12KE3). In this section, the characteristics of the two devices, considering thermal effects, are measured by the DPT.

The test bench of the DPT is usually adopted to test SiC (or Si) characteristics, as shown in Fig. 3. The DC power source (220 V) is assigned to a leg of the inverter and a pure inductor. One function/arbitrary waveform generator (Gigol DG1022) is used to output double pulses. The hot plate is used to boost the temperature of the devices; the maximum temperature can reach 300 °C. In

Please cite this article in press as: Ding X et al. Effects of silicon carbide MOSFETs on the efficiency and power quality of a microgrid-connected inverter. Appl Energy (2016), http://dx.doi.org/10.1016/j.apenergy.2016.10.011

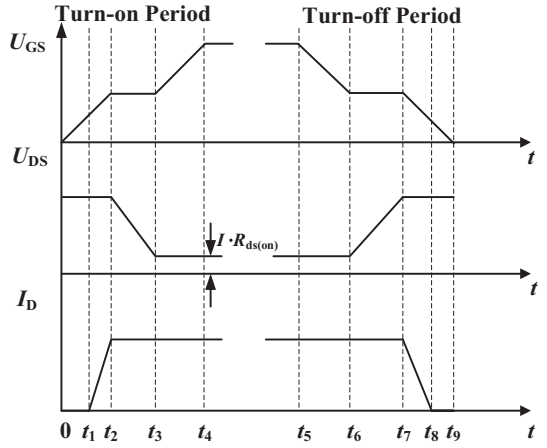

Fig. 4. Ideal switching transition waveforms.

addition, a current probe (Tektronix TCPA 300 plus TCP 303) and a voltage probe (Tektronix P5100A) with high accuracy are adopted to capture the current and voltage during the switching transient process. The fidelity of switching waveform is determined by the rise time of probes. The rise times of TCPA 300 plus TCP 303 and P5100A are 2.19 ns and 5.3 ns, which satisfy the demands of fast switching of SiC.

Ideal waveforms during the switching transition are shown in Fig. 4. U_{GS} is the voltage across the gate to the source; U_{DS} is the voltage across the drain to the source. I_D is the channel current through the SiC MOSFET. The systematic introduction of the switching transition is shown in our previous work [27]. However, because of stray inductance and capacitance in the circuit and the devices, the real current and voltage waveforms are different from the theoretical waveforms [28]. The waveforms are also affected by temperature. Therefore, to investigate the effect of the SiC MOSFET on the inverter, the real characteristics of the devices are measured firstly.

The switching transitions of SiC and Si at ambient temperature (25 °C) are shown in Figs. 5 and 6, respectively. The green line represents the voltage of the gate-source; the blue and red lines describe the drain-source voltage and drain current, respectively. Figs. 5a and 6a show the total switching transition waveforms for SiC and Si, respectively. Figs. 5b and 6b describe turn-off transitions, and Figs. 5c and 6c show turn-on transitions. Although the switching of SiC manifests a faster speed, both the current overshoot and voltage overshoot of SiC are higher than the counterparts of Si according to $i = C \cdot du/dt$ and $u = L \cdot di/dt$.

In addition, the switching time comparisons between SiC and Si at 25 °C are shown in Fig. 7. The figure clearly shows that both the turn-on time and the turn-off time of SiC are shorter than those of Si. The turn-on time of SiC is almost two thirds that of Si, and the turn-off time of Si is two times that of SiC.

Furthermore, the switching times of both SiC and Si are tested considering thermal effects. Fig. 8 shows the switching time of SiC MOSFETs at different temperatures. The time constant of the gate charge-discharge increases while the gate threshold voltage decreases with increasing temperature. Therefore, the turn-on and turn-off times of SiC are almost invariable under different temperatures [27]. The turn-off times of Si increase with increasing temperature, while the turn-on times remain constant, as shown in Fig. 9, consistent with the datasheet of Si [29].

In addition to the switching characteristics of the two devices, the voltage drops of the two devices are also measured considering the temperature. The results are shown in Table 1. The voltage drop of SiC increases with increasing temperature, while the voltage drop of Si decreases with increasing temperature. In addition, the other characteristics of both SiC and Si are shown in Table 2, including turn-on time, turn-off time, on-state resistance for SiC, collector-emitter saturation voltage for Si and output capacitance; these are vital for calculating the power losses and evaluating the power quality of SiC- and Si-inverters.

3. Microgrid-connected inverter power losses

This section will model and calculate the losses of both SiC- and Si-inverters according to DPT results, taking thermal effects into account. The power loss of a switching device consists of two parts: switching loss and conduction loss. A quantitative power loss analysis is based on the primary electrical characteristic parameters.

3.1. Switching energies

Both the turn-on and turn-off energies of switching SiC as functions of integration voltage and current during a commuted interval are shown as follows [29],

$$E_{T\_on} = \int_{t_1}^{t_2} V_{ds} \cdot I_d dt \tag{1}$$

$$E_{T\_off} = \int_{t_3}^{t_4} V_{ds} \cdot I_d dt \tag{2}$$

where E_{T_on} and E_{T_off} represent turn-on and turn-off energies, respectively. t_1, t_2, t_3 and t_4 denote the start and terminal turn-on and turn-off times, respectively. The switching energies of Si can be calculated the same as those of SiC.

3.2. Conduction losses

The conduction loss of a SiC MOSFET depends on the on-state resistance $R_{ds(on)}$ of the MOSFET; thus, the conduction loss expression is as simple as equation (3). V_{ds} is positively proportional to the temperature, as shown in Table 1. However, V_{ce} is negatively proportional to the temperature when the current is smaller than 100 A; this result is consistent with the datasheet of SiC [30].

$$P_{con} = I_d^2 \cdot R_{ds(on)} = V_{ds} \cdot I_d \tag{3}$$

3.3. Total losses of inverter

The expression of the switching losses of SiC MOSFETs and the diodes working under the ac line current, considering thermal effects, is derived from Ref. [31],

$$P_{ls}(T) = \frac{f_s}{\pi} \cdot (E_{T\_on}(T) + E_{T\_off}(T) + E_{off,D}(T)) \cdot \frac{U_{DC}}{V_{ref}} \cdot \frac{\sqrt{2} I_n}{I_{ref}} \tag{4}$$

where $n = 1$, indicating that $\sqrt{2}I_n$ is the peak value of the fundamental component of the ac line current for the motor with Y connected windings. V_{ref} and I_{ref} are the reference voltage and current, respectively. $E_{T\_on}(T)$ and $E_{T\_off}(T)$ are the turn-on and turn-off energies of SiC, separately taking thermal effects into account. $E_{off,D}(T)$ is the turn-off energy of the diode resulting from the reverse recovery current.

The conduction losses considering temperature can be derived from Ref. [32],

$$P_{lc,l}(T) = \sqrt{2}\left(\frac{1}{2\pi} + \frac{1}{8} a \cos\varphi\right) v_{ds0}(T) I_n + 2\left(\frac{1}{8} + \frac{1}{3\pi} a \cos\varphi\right) r_{ds}(T) I_n^2 \tag{5}$$

Please cite this article in press as: Ding X et al. Effects of silicon carbide MOSFETs on the efficiency and power quality of a microgrid-connected inverter. Appl Energy (2016), http://dx.doi.org/10.1016/j.apenergy.2016.10.011

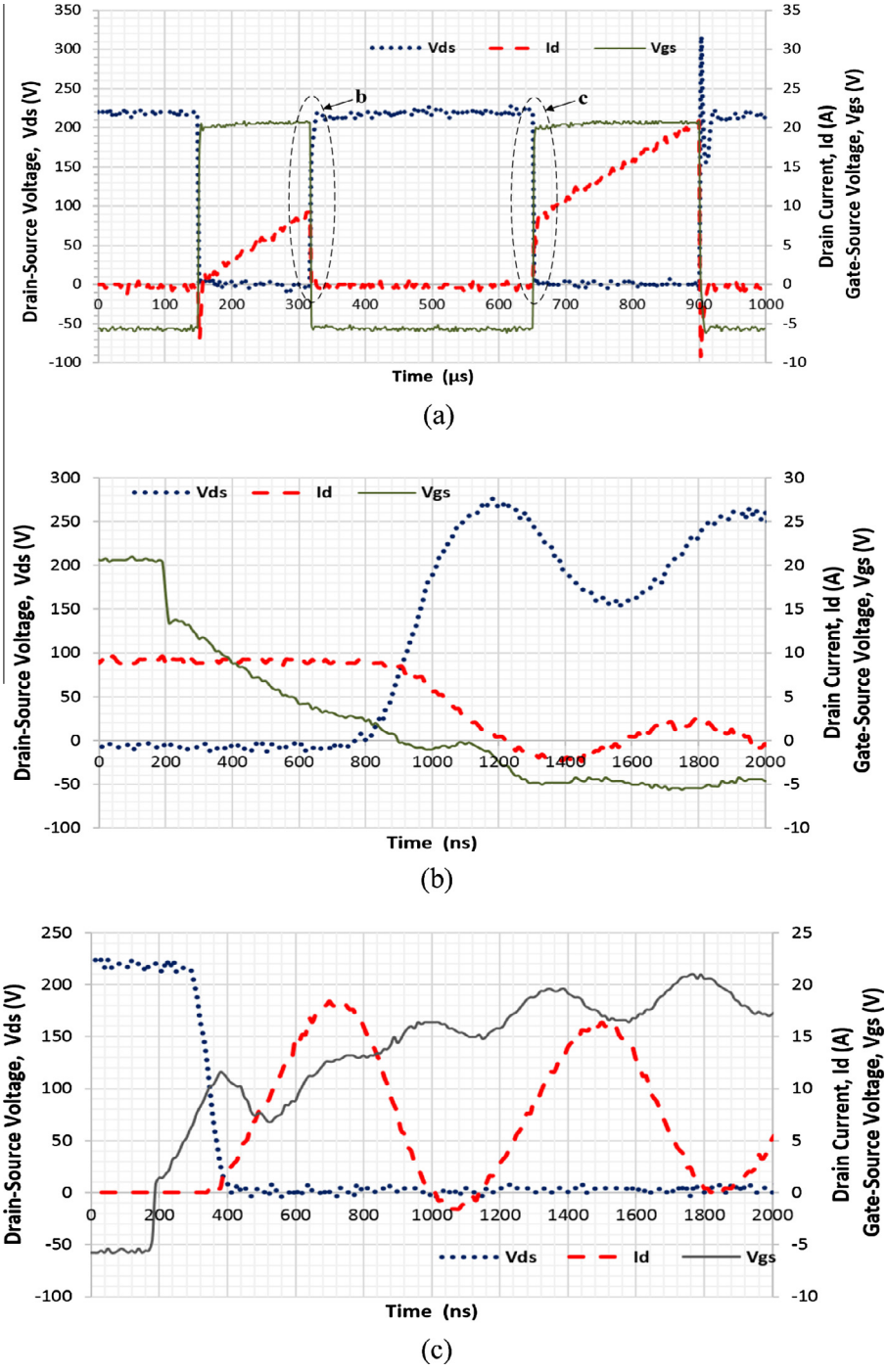

Fig. 5. Switching transition waveform of SiC. (a) Total switching transition; (b) turn-off transition; and (c) turn-on transition.

$$P_{\mathrm{lc,D}}(T) = \sqrt{2}\left(\frac{1}{2\pi} - \frac{1}{8}a\cos\varphi\right)v_{\mathrm{F0}}(T)I_{\mathrm{n}} + 2\left(\frac{1}{8} - \frac{1}{3\pi}a\cos\varphi\right)r_{\mathrm{F}}(T)I_{\mathrm{n}}^2 \quad (6)$$

where a and φ are the modulation index and power factor angle, respectively. $v_{\mathrm{ds0}}(T)$, $r_{\mathrm{ds}}(T)$, $v_{\mathrm{F0}}(T)$ and $r_{\mathrm{F}}(T)$ are on-state voltage drops and on-state resistances for the SiC MOSFET and diode considering temperature, respectively. Because there are six MOSFETs in an inverter, the total losses are given by

$$P_{\mathrm{in}}(T) = 6(P_{\mathrm{ls}}(T) + P_{\mathrm{lc,I}}(T) + P_{\mathrm{lc,D}}(T)) \quad (7)$$

3.4. Power losses calculation

According to Eqs. (1) and (2) and the voltage and current waveforms during a commuted interval measured by the DPT, the switching energies of both SiC and Si are calculated through integral computation in a software-MATLAB, as shown in Table 3. Both turn-on and turn-off energies of SiC are significantly smaller than the counterparts of Si. The turn-on energy of Si is increasing as temperature rising while the switching energies of SiC were almost constant. It is more robust to temperature as can be seen from Fig. 8 that the turn-on and turn-off times of SiC are almost invariable at different temperatures.

Please cite this article in press as: Ding X et al. Effects of silicon carbide MOSFETs on the efficiency and power quality of a microgrid-connected inverter. Appl Energy (2016), http://dx.doi.org/10.1016/j.apenergy.2016.10.011

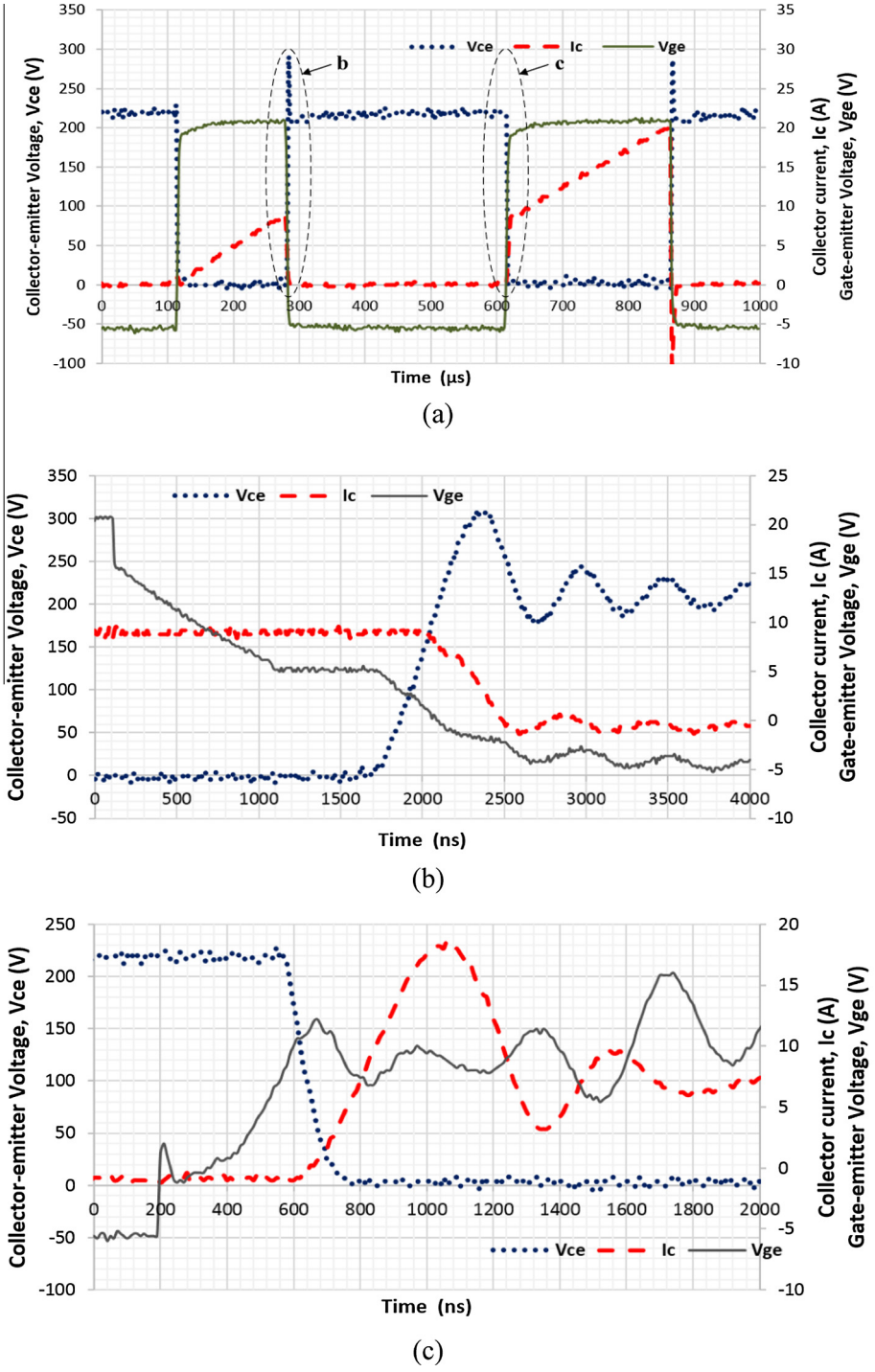

Fig. 6. Switching transition waveform of Si. (a) Total switching transition; (b) turn-off transition; and (c) turn-on transition.

Meanwhile, the conduction losses are calculated based on the measured voltage drops of the devices in Table 1 and equation (3). The results are shown in Table 4. The conduction losses of SiC are also smaller than the counterparts of Si. And the conduction losses of SiC increase with increasing temperature, while those of Si decrease. The results are consistent with the variation tendency of voltage drops.

4. Power quality analysis

The voltage distortion resulting from the non-ideal behavior of the commutation phenomena is analyzed in this section; this distortion will induce the harmonic components in the current. The three contributions are considered, such as dead time, voltage drops and switching delay times.

It is convenient to describe the voltage distortion effects from one phase leg of the inverter and extend the results to the other two phase legs. The one phase leg includes two switching devices S_{A_H} and S_{A_L}, two freewheeling diodes D_{A_H} and D_{A_L}. The phase current i_a is defined as positive when it flows into the motor, as shown in Fig. 10(a). The leg output current is assumed to be a constant value during the relatively short switching period according to the inductive behavior of the load.

Please cite this article in press as: Ding X et al. Effects of silicon carbide MOSFETs on the efficiency and power quality of a microgrid-connected inverter. Appl Energy (2016), http://dx.doi.org/10.1016/j.apenergy.2016.10.011

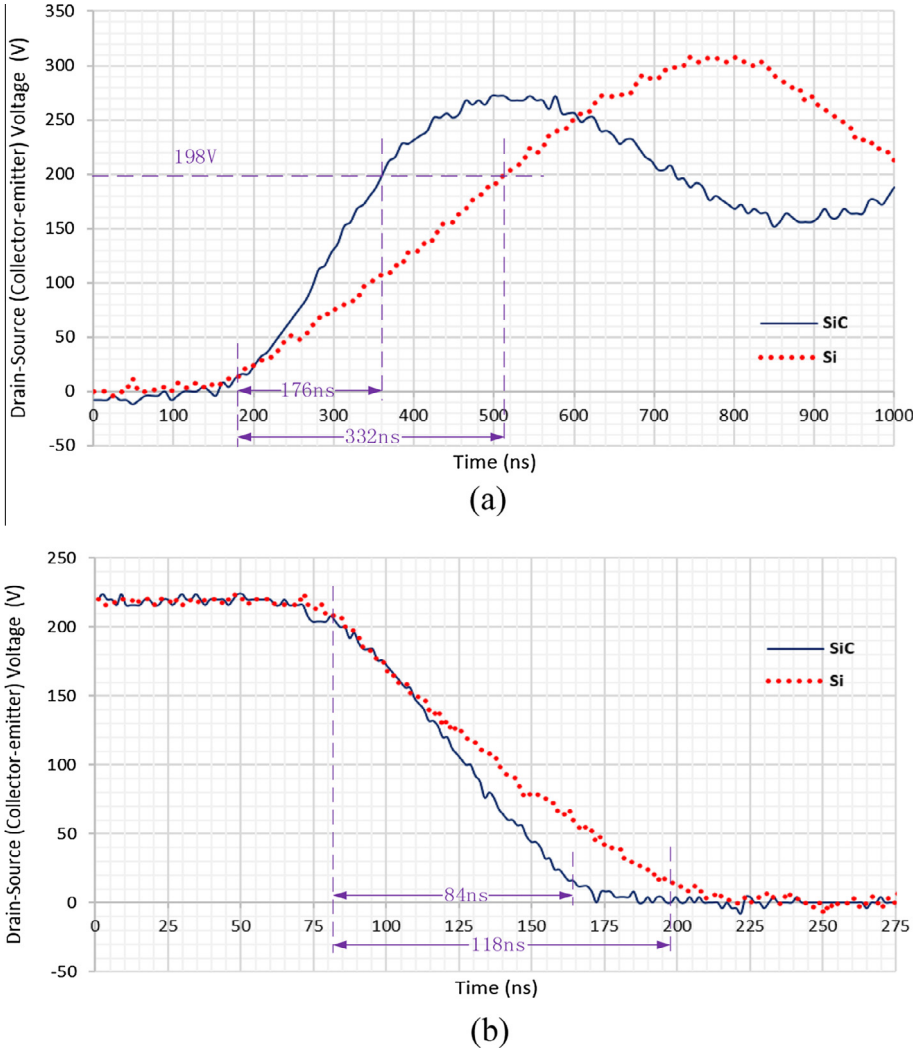

Fig. 7. Switching time comparisons between SiC and Si. (a) Turn-off time and (b) turn-on time.

The output phase voltage during switching time (T_S) when considering voltage drops, dead time and switching delay time effects is described in Fig. 11. The voltage errors (increase and decrease) between ideal and real switchings are highlighted by the colored areas and are identified by + and − signs. The dead time contribution is represented with a blue area, while the diode and MOSFET (or IGBT) effects are shown as green[1] and yellow areas, respectively. The turn-on and turn-off contribution delays are represented with red and purple areas, respectively.

For the MOSFET (or IGBT) and diode contributions, the average distortion voltage could be expressed as,

$$V_{err1} = -(V_T \cdot D + V_D \cdot (1 - D)) \cdot sign(i_a) \quad (8)$$

where V_T and V_D are the voltage drops of the MOSFET (or IGBT) and diode, respectively. D is the duty cycle,

$$sign(i_a) = \begin{cases} 1, & i_a > 0 \\ -1, & i_a < 0 \end{cases}.$$

For the dead time effect, the average distortion voltage also could be expressed as,

$$V_{err2} = (-T_{dt}/(2T_s)) \cdot V_{DC} \cdot sign(i_a) \quad (9)$$

where V_{DC} is the voltage of the DC power source. T_{dt} is the dead time, and T_s is the switching period.

For the switching delay time effect, the average distortion voltage also could be a function of the phase current sign,

$$V_{err3} = ((T_{d(off)} - T_{d(on)})/(2T_S)) \cdot V_{DC} \cdot sign(i_a) \quad (10)$$

where V_{DC} is the voltage of the DC power source. T_{dt} is the dead time, and T_s is the switching period.

Hence, the average voltage distortions of three phases can be expressed due to the direction of the three-phase currents separately as [33],

$$V_{aerr} = ((T_{d(off)} - T_{d(on)} - T_{dt})/(2T_s)) \cdot V_{DC} \cdot (1 - V_T D - V_D(1 - D)) \times \{(2sign(i_a) - sign(i_b) - sign(i_c))/3\} \quad (11)$$

$$V_{berr} = ((T_{d(off)} - T_{d(on)} - T_{dt})/(2T_s)) \cdot V_{DC} \cdot (1 - V_T D - V_D(1 - D)) \times \{(2sign(i_b) - sign(i_c) - sign(i_a))/3\} \quad (12)$$

$$V_{cerr} = ((T_{d(off)} - T_{d(on)} - T_{dt})/(2T_s)) \cdot V_{DC} \cdot (1 - V_T D - V_D(1 - D)) \times \{(2sign(i_c) - sign(i_a) - sign(i_b))/3\} \quad (13)$$

Therefore, the average distorted voltage over the entire cycle of the current can be plotted as six-step waveform in Fig. 12. The voltage is 180° out of phase with the phase current.

[1] For interpretation of color in Fig. 11, the reader is referred to the web version of this article.

Please cite this article in press as: Ding X et al. Effects of silicon carbide MOSFETs on the efficiency and power quality of a microgrid-connected inverter. Appl Energy (2016), http://dx.doi.org/10.1016/j.apenergy.2016.10.011

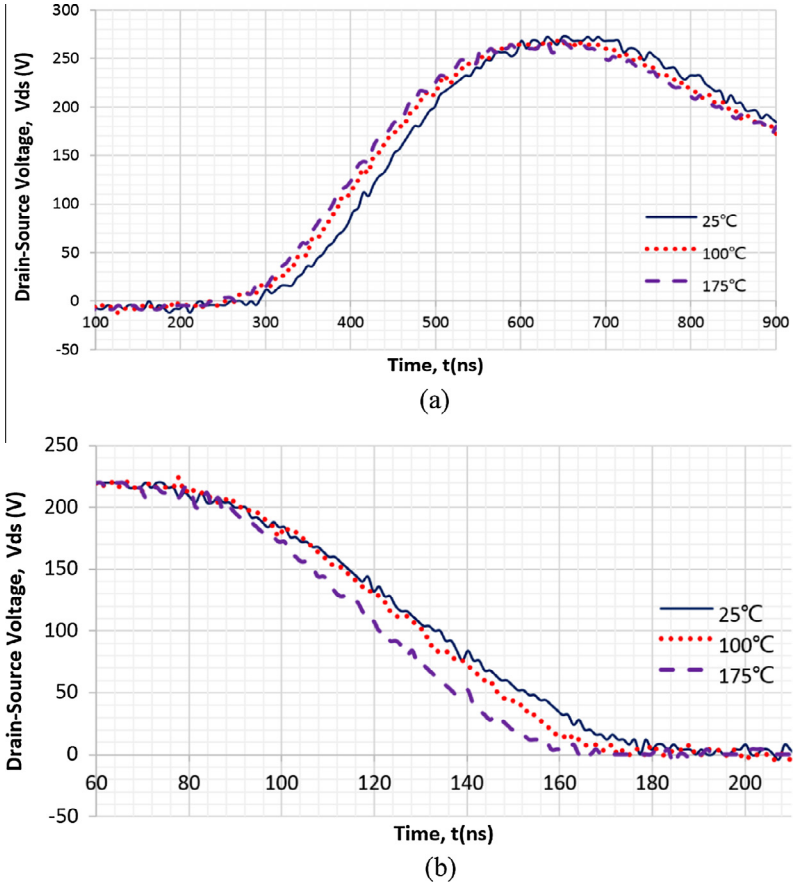

Fig. 8. Switching time of SiC MOSFETs at different temperatures. (a) Turn-off time and (b) turn-on time.

Fig. 13 represents how the distorted voltage affects the power quality of the inverter output voltage. If there were no voltage drops, dead time and time delays, the fundamental output voltage of the inverter can be described as V_{ref}. The current i lags behind V_{ref} by an angle θ' if the load is inductive, such as motor, inductance. Fig. 12 shows the distorted voltage V_{aeer} increases (decreases) the output phase voltage of the inverter for the negative (positive) half cycle of the current. The fundamental component of the voltage distortion is defined as V_{aeer1} shown in Fig. 13. The superposition of V_{aerr} on the fundamental voltage V_{ref} is shown as broken line. Therefore, the fundamental output voltage V_1 of the inverter with distorted voltage can be described as a heavy solid line. It is worth to mention that the real fundamental output voltage V_1 is different from the reference one V_{ref} in both the phase and magnitude. The phase displacement θ between V_1 and i becomes bigger than the reference one θ'. And the magnitude of the voltage V_1 is smaller than $V_{ref.}$ The distorted voltage also induces more harmonics in the phase current due to the current directly depending on the output voltage of the inverter with voltage-controlled device, namely IGBTs and MOSFETs.

According to the characteristics of SiC and Si shown in Table 2, the average distorted voltages effected by the three contributions are calculated based on the previous equations, as shown in Table 5. The average distorted voltages of SiC are smaller than those of Si at both an ambient temperature of 25 °C and a high temperature of 175 °C; these distorted voltages benefit from the advantages of SiC shown in Table 2, such as a higher switching speed, a lower on-resistance, and smaller dead time.

5. Experiments and model verification

Fig. 14 shows the test setup. The input of the inverter is connected to a DC power source with a voltage ranging from 0 to 300 V. A permanent magnet synchronous motor is used as the load of the inverter. A power analyzer is adopted to measure the input and output power of the inverter. Additionally, the phase current and voltage are also captured by high accuracy voltage and current probes (TCPA 300 plus TCP 303, P5100A) combined with an oscilloscope.

5.1. Inverter efficiency

The switching and conduction losses are calculated by expression (4) and expressions (5) and (6), respectively. Both the input power and output power of the inverter are measured by the power analyzer simultaneously.

The calculated total losses can be validated by experimental results for both SiC and Si under two different temperature conditions, as shown in Table 6. The experimental results are a little higher than the calculated ones according to the stray inductances and capacitances, increasing the turn-on and turn-off times [28]. However, in the worst situation, the error between the calculations and experiments is less than 15%. Meanwhile, though the switching loss of SiC and conduction loss of Si are negative proportional to the temperature, the total losses of both SiC and Si increase at elevated temperature.

Fig. 15(a) and (b) illustrates the power loss and energy conversion efficiency of the two inverters, respectively. Obviously, a SiC-MOSFET based inverter presents a lower power loss and a higher

Please cite this article in press as: Ding X et al. Effects of silicon carbide MOSFETs on the efficiency and power quality of a microgrid-connected inverter. Appl Energy (2016), http://dx.doi.org/10.1016/j.apenergy.2016.10.011

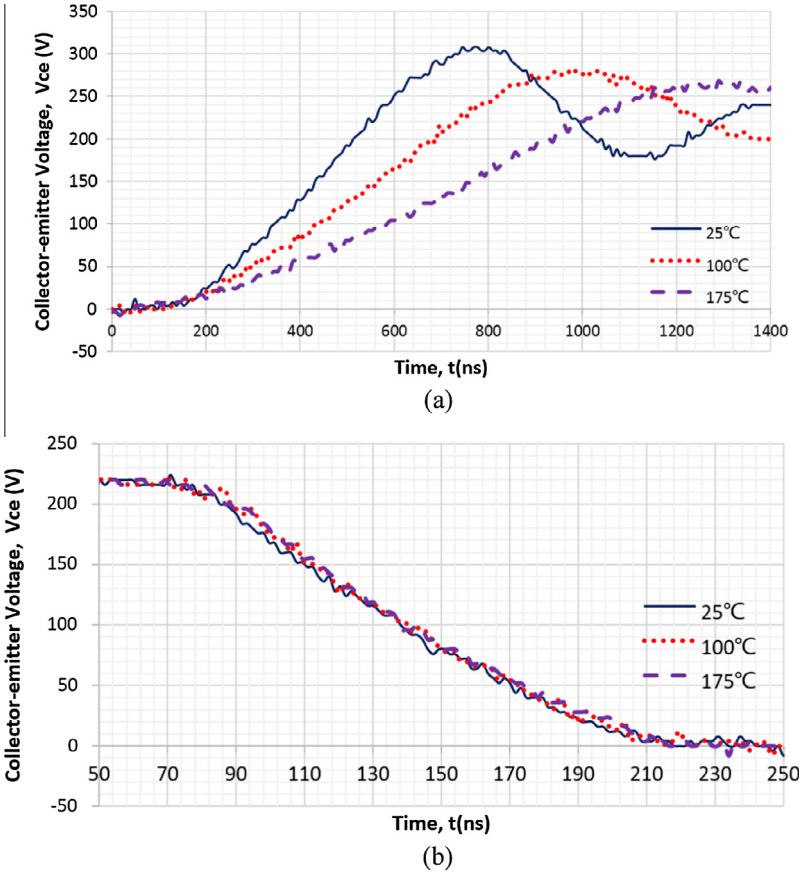

Fig. 9. Switching time of Si IGBT at different temperatures. (a) Turn-off time and (b) turn-on time.

Table 1
Voltage drops of SiC and Si under different temperatures.

Temperature (°C)	SiC (Cree CAS300M12BM2)		Si (Infineon FF400R12KE3)	
	V_{ds} (mV)	I_d (A)	V_{ce} (mV)	I_d (A)
25	44.2	9.2	832.5	9.5
100	60.1	9.2	686.9	9.3
175	73.7	9.4	583.0	9.4

efficiency compared with a Si-IGBT based inverter at a 220 V DC bus. The application of SiC devices will greatly reduce the power loss and improve the efficiency of microgrid systems. This opens up opportunities for greater system design optimization, such as determining the smallest possible power converter volume and weight.

5.2. Power quality

The phase currents of both SiC-MOSFET based inverters and Si-IGBT based inverters are measured and compared by experiments. Fig. 16 shows the phase current waveforms of Si-IGBT and SiC-MOSFET based inverters at 25 °C. Compared with Si-IGBT based inverters, the harmonic components in the phase current

Table 3
Switching energies of SiC and Si.

	Turn-on energy (μJ)		Turn-off energy (μJ)	
	Si IGBT	SiC MOSFET	Si IGBT	SiC MOSFET
25 °C	36.1	2.5	660.0	259.2
100 °C	34.3	2.5	1288.0	255.2
175 °C	33.6	2.4	1430.0	245.3

Table 4
Conduction losses of SiC and Si.

Temperature (°C)	SiC MOSFET (W)	Si IGBT (W)
25	0.40664	7.90875
100	0.55292	6.38817
175	0.69278	5.4802

Table 2
Characteristics of SiC and Si measured by the DPT.

	SiC (Cree CAS300M12BM2)		IGBT (Infineon FF400R12KE3)	
	25 °C	175 °C	25 °C	175 °C
DC voltage	220 V	220 V	220 V	220 V
Turn-on time	84 ns	78 ns	118 ns	120 ns
Turn-off time	176 ns	170 ns	332 ns	732 ns
On-state resistance	4.8 mΩ	7.84 mΩ	/	/
Collector-emitter saturation voltage	/	/	832.5 mV (9.5 A)	583.0 mV (9.4 A)
Output capacitance	12.7 nF	13.4 nF	32.7 nF	35.3 nF

Please cite this article in press as: Ding X et al. Effects of silicon carbide MOSFETs on the efficiency and power quality of a microgrid-connected inverter. Appl Energy (2016), http://dx.doi.org/10.1016/j.apenergy.2016.10.011

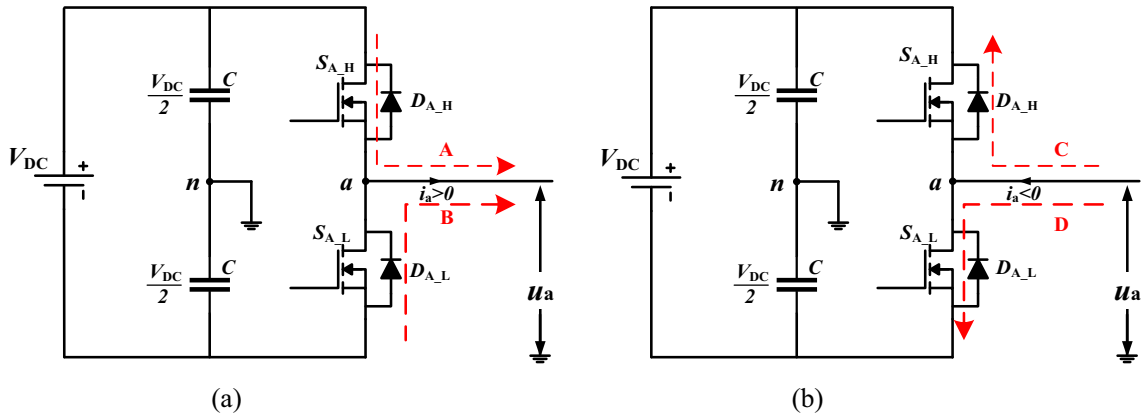

Fig. 10. One phase leg of an inverter. (a) Positive current flows into the motor. (b) Negative current flows into the phase leg.

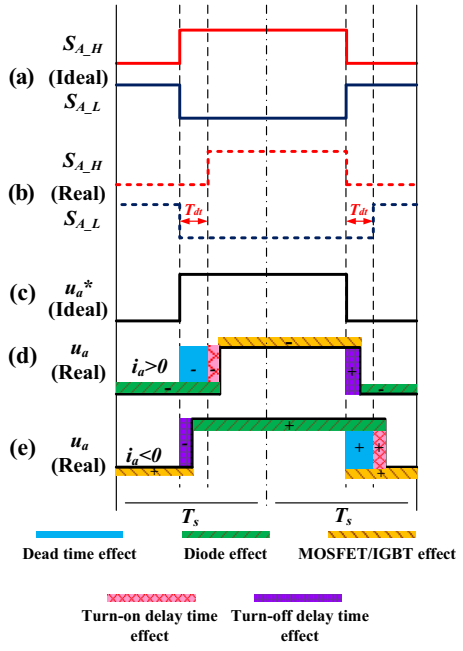

Fig. 11. Output voltage waveform during dead time taking voltage drops, dead time and switching delay time effects into account.

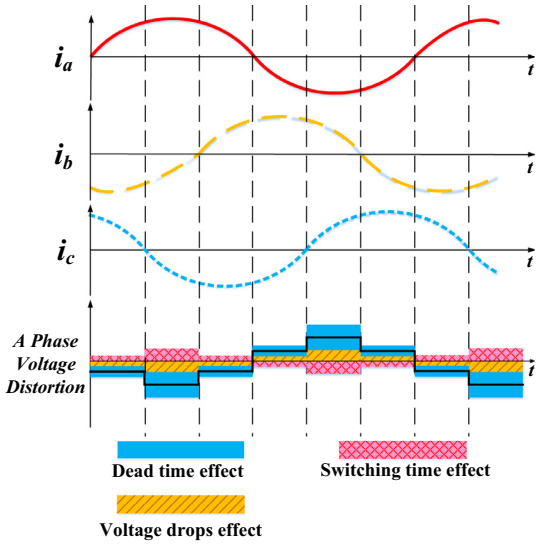

Fig. 12. The distorted voltage and three-phase currents.

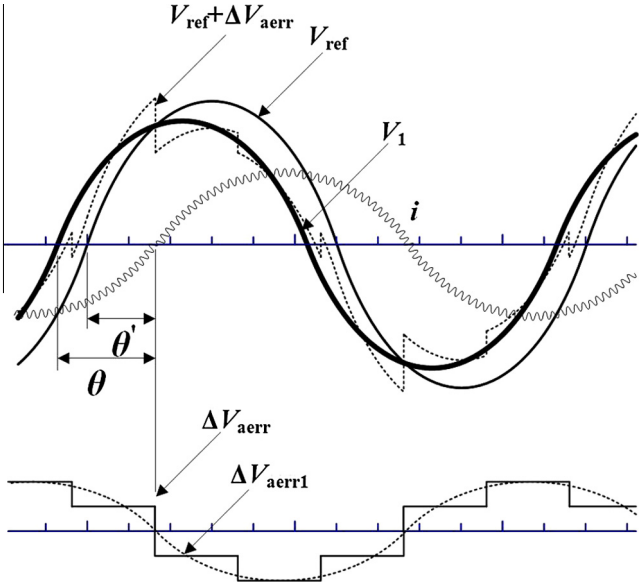

Fig. 13. The effect of voltage distortion on output phase voltage.

of the inverter based on SiC MOSFETs are smaller; this result is consistent with the analytical results shown in Table 5. When the amplitude of the fundamental component of the phase current is approximately 9 A, namely, I_1 = 9 A, the total harmonic distortion (THD) of the phase current in the SiC-inverter is 3.82%, while that in the Si-inverter is more than 11%. Furthermore, the THD of the phase of the SiC-inverter is only 3.07%, while the value of the Si-inverter is 5.66% when the inverter operates with approximately 18 A of the amplitude for the fundamental waveform. The higher power quality of the SiC-inverter should be the result of the high switching speed, lower on-resistance, smaller dead time of the SiC-inverter; these are explored in Section 2. This smaller THD of the SiC inverter also means that the size and weight of the filler used in the SiC-MOSFET systems is smaller than that in the Si-IGBT system.

Fig. 17 shows the phase current waveforms of Si-IGBT and SiC-MOSFET based inverters at 100 °C. As the same as the system operating at 25 °C, the THD of SiC-inverter is smaller than that of Si system with 100 °C operation temperature. Meanwhile, the THD of both SiC and Si-inverter decreases when the temperature increases, which validates the analytical results in Table 5. The average distorted voltages become smaller as temperature increase.

Please cite this article in press as: Ding X et al. Effects of silicon carbide MOSFETs on the efficiency and power quality of a microgrid-connected inverter. Appl Energy (2016), http://dx.doi.org/10.1016/j.apenergy.2016.10.011

Table 5
Average distorted voltages effected by the four contributions.

	25 °C				175 °C			
	SiC MOSFETs (V)	Si IGBTs (V)	Differences (V)	Percentage (%)	SiC MOSFETs (V)	Si IGBTs (V)	Differences (V)	Percentage (%)
Dead time effect	−1.65	−2.20	−0.55	25	−1.65	−2.20	−0.55	25
Switching delay time effect	0.10	0.24	0.14	58.3	0.14	0.31	0.17	54.8
Voltage drop effect	−0.87	−1.32	−0.45	34.1	−0.89	−1.20	−0.31	25.8
Total effects	−2.42	−3.28	−0.86	26.2	−2.4	−3.09	−0.69	22.3

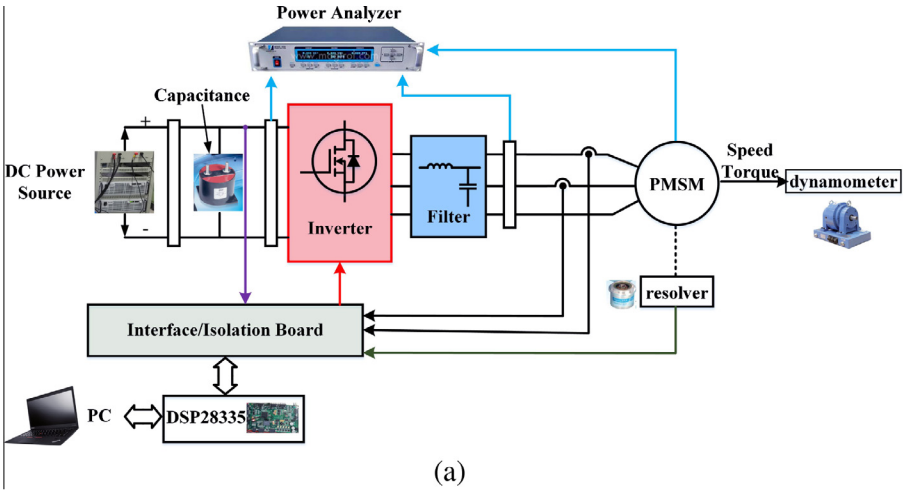

Fig. 14. Test setup. (a) Simplified schematic of the test setup. (b) Actual components in the test setup.

Table 6
Loss comparison between calculation and experiment.

	Temperature (°C)	Inverter output power (kW)	Calculated switching loss (W)	Calculated conduction loss (W)	Calculated total loss (W)	Experiment total losses (W)	Error (%)
SiC MOSFET	25	1	31.67	23.58	55.25	62	10.9
		3	54.69	31.01	85.70	91	5.8
	100	1	31.18	32.06	63.24	69	8.8
		3	53.85	42.16	96.01	103	7.3
Si IGBT	25	1	60.11	45.17	105.28	123	14.4
		3	133.27	63.72	196.99	211	6.6
	100	1	104.18	36.48	140.66	158	12.9
		3	213.15	51.47	264.62	286	8.4

Please cite this article in press as: Ding X et al. Effects of silicon carbide MOSFETs on the efficiency and power quality of a microgrid-connected inverter. Appl Energy (2016), http://dx.doi.org/10.1016/j.apenergy.2016.10.011

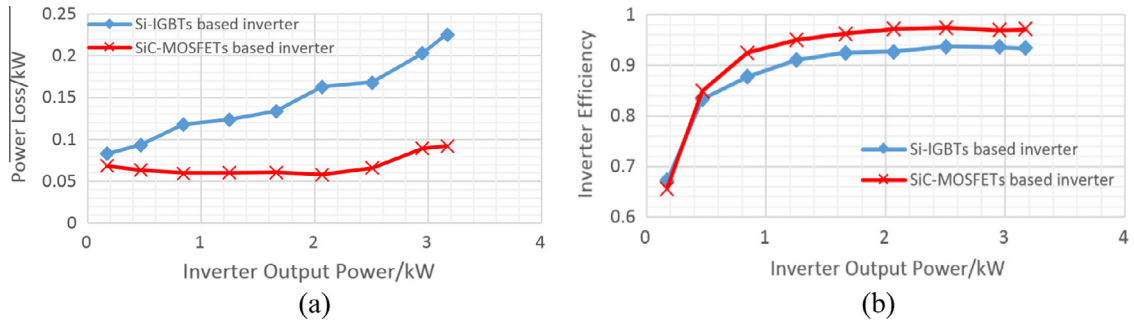

Fig. 15. (a) Power loss comparison of Si-IGBT and SiC-MOSFET based inverters at a 220 V DC bus; (b) Efficiency comparison of Si-IGBT and SiC-MOSFET based inverters at a 220 V DC bus.

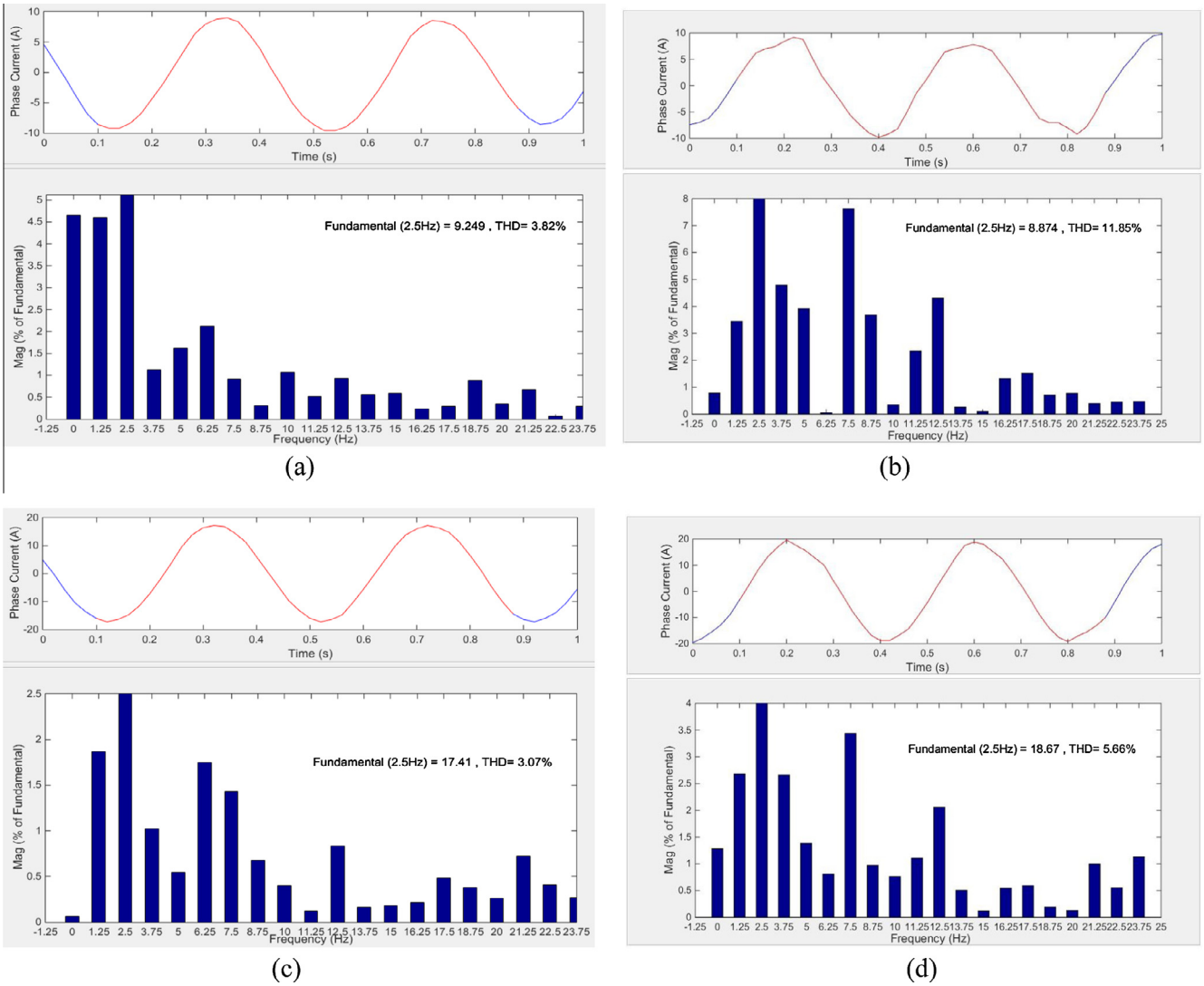

Fig. 16. Phase current waveforms of SiC and Si based inverters at 25 °C. (a) Phase current of SiC inverter with almost 9 A; (b) phase current of Si inverter with almost 9 A; (c) phase current of SiC inverter with almost 18 A; and (d) phase current of Si inverter with almost 18 A.

Fig. 13 shows that the distorted voltage will reduce the amplitude of the phase voltage. In addition, the distorted voltage of Si is larger than SiC. Therefore, compared with SiC based system, the amplitude of the fundamental phase voltage for Si based system is smaller. In order to achieve the same output power with SiC system, the phase current of Si-system needs to increase to compensate for the loss of the phase voltage and power factor. Both Figs. 16 and 17 support this conclusion. It can be observed that the phase-current amplitudes of Si-inverter are higher than the counterparts of SiC-inverter in Figs. 16 and 17.

Please cite this article in press as: Ding X et al. Effects of silicon carbide MOSFETs on the efficiency and power quality of a microgrid-connected inverter. Appl Energy (2016), http://dx.doi.org/10.1016/j.apenergy.2016.10.011

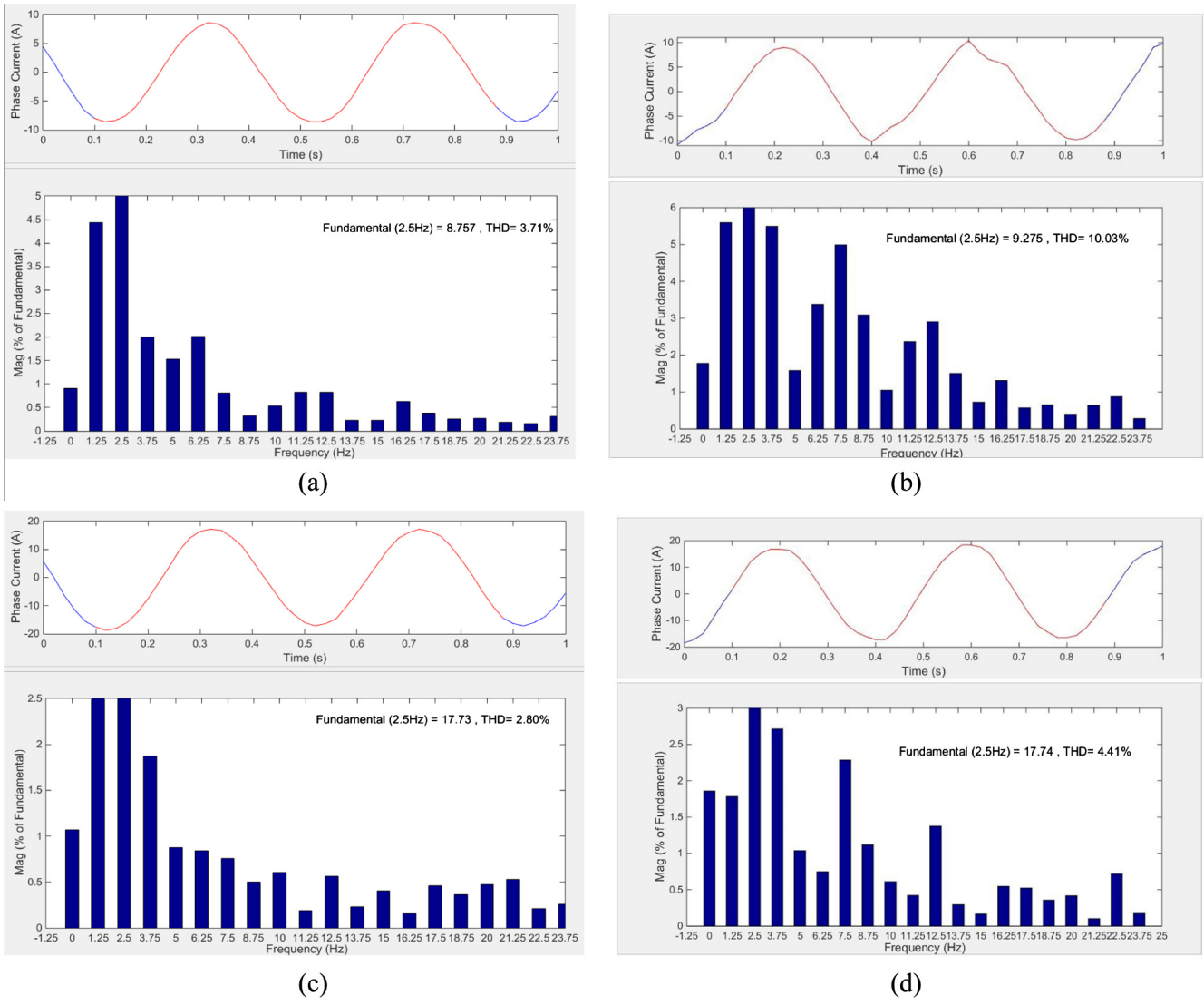

Fig. 17. Phase current waveforms of SiC and Si based inverters at 100 °C. (a) Phase current of SiC inverter with almost 9 A; (b) phase current of Si inverter with almost 9 A; (c) phase current of SiC inverter with almost 18 A; and (d) phase current of Si inverter with almost 18 A.

6. Conclusions

This paper discussed the power loss and quality of the inverter based on SiC-MOSFETs and compared it with Si-IGBT based inverters, particularly from the viewpoint of the characteristics of SiC. The behavior of SiC was measured by the DPT considering thermal effects and manifested its intrinsic advantages, such as a fast switching speed and a low voltage drop. Both the switching energies and conduction losses of SiC are smaller than those of Si at different temperatures. The switching energies of SiC decrease slightly as the temperature increases, while the Si counterparts increase tremendously with increasing temperature. Such a scenario is different than that for the conduction losses. Furthermore, considering temperature effects, the losses of SiC- and Si-inverters were modeled and validated by an experiment. Additionally, compared with Si inverters, the SiC-MOSFET inverter has less harmonic current in microgrids; harmonic current was measured and validated through an experiment.

Because of the ability to increase the energy efficiency and improve the power quality, SiC devices are expected to be broadly applicable for microgrids. However, the cost, electromagnetic interference (EMI) and high power rating of SiC MOSFETs should be solved before SiC MOSFETs replaces Si IGBTs in microgrid applications. It can be predicted that the excellent performance of SiC power devices could significantly impact the power grid in various aspects, such as improvements in power density, cooling requirements, system response times, overload capability, and reliability.

Acknowledgments

This work was supported in part by the National Natural Science Foundation of China under Project 51407004 and in part by the Aeronautical Science Foundation of China 2013ZC51031.

References

[1] Xiong R, Sun F, Chen Z, He H. A data-driven multi-scale extended Kalman filtering based parameter and state estimation approach of lithium-ion polymer battery in electric vehicles. Appl Energy 2014;113(Jan.):463–76.
[2] Zhang S, Xiong R, Cao JY. Battery durability and longevity based power management for plug-in hybrid electric vehicle with hybrid energy storage system. Appl Energy 2016;179(Oct):316–28.
[3] Shamsi P, Fahimi B. Stability assessment of a DC distribution network in a hybrid micro-grid application. IEEE Trans Smart Grid 2014;5(5):2527–34.

Please cite this article in press as: Ding X et al. Effects of silicon carbide MOSFETs on the efficiency and power quality of a microgrid-connected inverter. Appl Energy (2016), http://dx.doi.org/10.1016/j.apenergy.2016.10.011

[4] Blaabjerg F, Iov F, Terekes T, et al. Power electronics-key technology for renewable energy systems. In: 2nd Power electronics drive systems and technologies conference (PEDSTC), 2011. IEEE; 2011. p. 445–66.
[5] Stadler M, Cardoso G, Mashayekh S, et al. Value streams in microgrids: a literature review. Appl Energy 2016;162:980–9.
[6] Sun F, Xiong R, He H. A systematic state-of-charge estimation framework for multi-cell battery pack in electric vehicles using bias correction technique. Appl Energy 2016;162(January):1399–409.
[7] Patrao I, Garcerá G, Figueres E, et al. Grid-tie inverter topology with maximum power extraction from two photovoltaic arrays. IET Renew Power Gener 2014;8(6):638–48.
[8] Zhou Y, Huang W, Zhao P, et al. A transformerless grid-connected photovoltaic system based on the coupled inductor single-stage boost three-phase inverter. IEEE Trans Power Electron 2014;29(3):1041–6.
[9] Zhang S, Xiong R. Adaptive energy management of plug-in hybrid electric vehicle based on driving pattern recognition and dynamic programming. Appl Energy 2015;155(August):68–78.
[10] Meneses D, Blaabjerg F, Garcia O, et al. Review and comparison of step-up transformerless topologies for photovoltaic AC-module application. IEEE Trans Power Electron 2013;28(6):2649–63.
[11] Kranzer D, Wilhelm C, Reiners F, et al. Application of normally-off SiC-JFETs in photovoltaic inverters. 2009 13th European conference on power electronics and applications 2009.
[12] Rabkowski J, Peftitsis D, Nee HP. Design steps toward a 40-kVA SiC JFET inverter with natural-convection cooling and an efficiency exceeding 99.5%. IEEE Trans Ind Appl 2013;49(4):1589–98.
[13] Burger B, Kranzer D, Stalter O. Cost reduction of PV-inverters with SiC-DMOSFETs. In: 2008 5th International conference on integrated power systems (CIPS), VDE. p. 1–5.
[14] Khadem M, Basu M, Conlon MF. UPQC for power quality improvement in DG integrated smart grid network–a review. J Emerg Electr Power Syst 2012;13:3.
[15] 5th Ceer benchmarking report on the quality of electricity supply. Council of European Regulator, April 2012 <www.energy-regulators.eu>.
[16] Basak P, Chowdhury S, Halder nee Dey S, Chowdhury SP. A literature review on integration of distributed energy resources in the perspective of control protection and stability of microgrid. Renew Sustain Energy Rev 2012;16 (8):5545–56.
[17] IEEE application guide for IEEE Std 1547. IEEE standard for interconnecting distributed resources with electric power systems. IEEE Std 1547.2-2008; 2009. p. 1–217.
[18] IEEE recommended practice and requirements for harmonic control in electric power systems. IEEE Std 519–2014 (revision IEEE Std 519–1992); 2014. p. 1–29.
[19] Palizban O, Kauhaniemi K, Guerrero JM. Microgrids in active network management–part II: system operation, power quality and protection. Renew Sustain Energy Rev 2014;36:440–51.
[20] Carrasco JM et al. Power-electronic systems for the grid integration of renewable energy sources: a survey. Ind Electron IEEE Trans 2006;53:1002–16.
[21] Li YW, Vilathgamuwa DM, Loh PC. A grid-interfacing power quality compensator for three-phase three-wire microgrid applications. IEEE 35th annual power electronics specialists conference, vol. 3. p. 2011–7.
[22] Li YW, Vilathgamuwa DM, Loh PC. Microgrid power quality enhancement using a three-phase four-wire grid-interfacing compensator. IEEE Trans Ind Appl 2005;41(6):1707–19.
[23] Khadem SK et al. A review of parallel operation of active power filters in the distributed generation system. In: Proceedings of the2011-14th European conference on power electronics and applications (EPE). p. 1–10.
[24] Chakraborty S, Weiss MD, Simoes MG. Distributed intelligent energy management system for a single-phase high-frequency AC microgrid. IEEE Trans Ind Electron 2007;54(1):97–109.
[25] Khadem SK, Basu M, Conlon MF. A review of parallel operation of active power filters in the distributed generation system. In: 14th European conference on power electronics and applications (EPE). p. 1–10.
[26] Tzung-Lin L, Po-Tai C. Design of a new cooperative harmonic filtering strategy for distributed generation interface converters in an islanding network. IEEE Trans Power Electron 2007;22(5):1919–27.
[27] Xiaofeng Ding, Min Du, Tong Zhou, et al. Comprehensive comparison between silicon carbide MOSFETs and silicon IGBTs based traction systems for electric vehicles. Appl Energy 2016. doi: http://dx.doi.org/10.1016/j.apenergy.2016.05.059.
[28] Zhang Z, Wang F, Tolbert LM, Blalock BJ, Costinett DJ. Evaluation of switching performance of SiC devices in PWM inverter-fed induction motor drives. IEEE Trans Power Electron 2015;30(10):5701–11.
[29] Chen Hsin-Ju, Kusic George L, Reed Gregory F. Comparative PSCAD and Matlab/Simulink simulation models of power losses for SiC MOSFET and Si IGBT devices. In: Power and energy conference at Illinois (PECI), 2012. IEEE. p. 1–5.
[30] http://www.alldatasheet.com/datasheet-pdf/pdf/165427/EUPEC/FF400R12KE3.html.
[31] Hassan W, Wang B. Efficiency optimization of PMSM based drive system. 7th International power electronics and motion control conference (IPEMC), 2012, vol. 2. IEEE; 2012.
[32] Mestha LK, Evans PD. Analysis of on-state losses in PWM inverters. Electr Power Appl, IEE Proc B 1989;136(4):189–95.
[33] Choi JW, Sul SK. Inverter output voltage synthesis using novel dead time compensation. IEEE Trans Power Electron 1996;11(2):221–7.

Please cite this article in press as: Ding X et al. Effects of silicon carbide MOSFETs on the efficiency and power quality of a microgrid-connected inverter. Appl Energy (2016), http://dx.doi.org/10.1016/j.apenergy.2016.10.011